Low-dimensional chaos in zero-Prandtl-number Bénard–Marangoni convection

Thomas Boeck[1] and Nikolay K. Vitanov[1,2]
[1]*Max-Planck-Institute for Physics of Complex Systems, Nöthnitzer Strasse 38, 01187 Dresden, Germany*
[2]*Institute of Mechanics, Bulgarian Academy of Sciences, Acad. G. Bonchev Street, Block 4, 1113, Sofia, Bulgaria*
(Received 6 July 2001; published 7 March 2002)

Three-dimensional surface-tension-driven Bénard convection at zero Prandtl number is computed in the smallest possible doubly periodic rectangular domain that is compatible with the hexagonal flow structure at the linear stability threshold of the quiescent state. Upon increasing the Marangoni number beyond this threshold, the initially stationary flow becomes quickly time dependent. We investigate the transition to chaos for the case of a free-slip bottom wall by means of an analysis of the kinetic energy time series. We observe a period-doubling scenario for the transition to chaos of the energy attractor, intermittent behavior of a component of the mean velocity field, three characteristic energy levels, and two frequencies that contain a considerable amount of the power spectral density connected with the kinetic energy time series.

DOI: 10.1103/PhysRevE.65.037203 PACS number(s): 05.45.Ac, 47.20.Dr, 47.27.Te

Most experimental and theoretical works on surface-tension-driven Bénard convection (also called Bénard-Marangoni convection or BMC for short) deal with high-Prandtl-number fluids [1,2] of large viscosity showing either stationary or weakly time-dependent flows of small Reynolds number. BMC in low-Prandtl-number fluids (liquid metals) has received far less attention although surface-tension-driven convection of liquid metals, plays an important role in industrial processes such as crystal growth [2] or electron beam evaporation [3,4]. In these applications, the Reynolds number is large and the flow, therefore, time dependent or even turbulent due to the strong thermal forcing and the relatively low viscosity. Liquid metals are not transparent and thus, difficult for experimental investigation. Therefore, numerical simulations are commonly used to study geometries that resemble actual experimental or industrial setups [5–7]. Simulations at low Prandtl numbers for the geometrically simple Bénard configuration have only been performed recently [8,9]. This paper extends the systematic study of low-Prandtl-number BMC described in Ref. [9]. Similar to work on Rayleigh-Bénard convection [10], the focus is on the transition between convection with regular time dependence and convection with chaotic time dependence occurring when the heating is increased.

We consider a horizontal planar layer of incompressible Newtonian fluid heated from below under the assumptions of a nondeflecting free upper surface, and of a driving of the convective flow by the surface tension forces only. Neglecting buoyancy is justified if the layer is sufficiently thin or under microgravity conditions. The isothermal bottom [11] of the layer coincides with $z=0$. We choose the layer thickness d as the unit of length and denote by L_x and L_y the (dimensionless) periodicity intervals corresponding to the periodic x and y directions. Next we introduce the deviation θ from the the conductive temperature profile defined by $T=\theta+T_{bottom}-\Delta T_0 z$, and prescribe the heat flux density at the free surface, i.e., $\partial_z\theta=0$. The tangential force balance at the free surface requires that $\rho\nu(\partial\mathbf{v}/\partial z)=\boldsymbol{\nabla}\sigma$, where $\mathbf{v}$ denotes the velocity, ρ the density, and ν the kinematic viscosity. The surface tension decreases with temperature as $\sigma=\sigma(T_r)-\gamma(T-T_r)$, where T_r stands for a reference temperature. Using ν/d as the unit for velocity, d^2/ν as the unit for time, $\nu\Delta T_0/\kappa$ as the unit of θ (κ denotes the thermal diffusivity) we obtain the dimensionless equations in the case of zero Prandtl number $Pr=\nu/\kappa$,

$$\partial\mathbf{v}/\partial t+(\mathbf{v}\cdot\boldsymbol{\nabla})\mathbf{v}=-\boldsymbol{\nabla}p+\nabla^2\mathbf{v}, \tag{1}$$

$$\boldsymbol{\nabla}\cdot\mathbf{v}=0, \tag{2}$$

$$\nabla^2\theta+v_z=0, \tag{3}$$

together with the conditions $\partial v_x/\partial z+Ma(\partial\theta/\partial x)=\partial v_y/\partial z+Ma(\partial\theta/\partial y)=v_z=\partial\theta/\partial z=0$ at $z=1$ and $\partial v_x/\partial z=\partial v_y/\partial z=v_z=\theta=0$ at $z=0$, and with the Marangoni number $Ma=\gamma\Delta T_0 d/(\rho\nu\kappa)$ as the control parameter.

The evolution equations (1)–(3) are solved by the pseudospectral numerical method of Ref. [9], which is based on Fourier series in x and y coordinates and a Chebyshev polynomial expansion in the z coordinate [12–14]. All runs reported below were performed on a Cray T3E parallel computer with the same set of initial velocity and temperature data (converged state for $Ma=65$). The numerical parameters used were as follows: time step $\Delta t=2\times10^{-4}$, 64×32 Fourier modes, and 33 Chebyshev polynomials. The total (single processor) computing time amounted to 10 000 hours.

For periodic boundary conditions, the smallest rectangular periodicity domain compatible with the hexagonal pattern has the size $L_x=4\pi/k_c$, $L_y=4\pi/(\sqrt{3}k_c)$. Below we shall consider this domain with a wave number $k_c=1.70$ corresponding to the linear instability threshold $Ma_c=57.6$ of the basic state of pure heat conduction [8]. The hexagonal convection pattern appears subcritically at Ma_c and persists down to $Ma\approx57.0$. For $Ma>59.5$ it is replaced by deformed hexagons. The kinetic energy for this state remain almost constant up to the onset of time-dependent convection through an oscillatory instability at $Ma\approx63$. This new state is characterized by an oscillating deformed hexagon and the formation and decay of a roll-like structure in the computa-

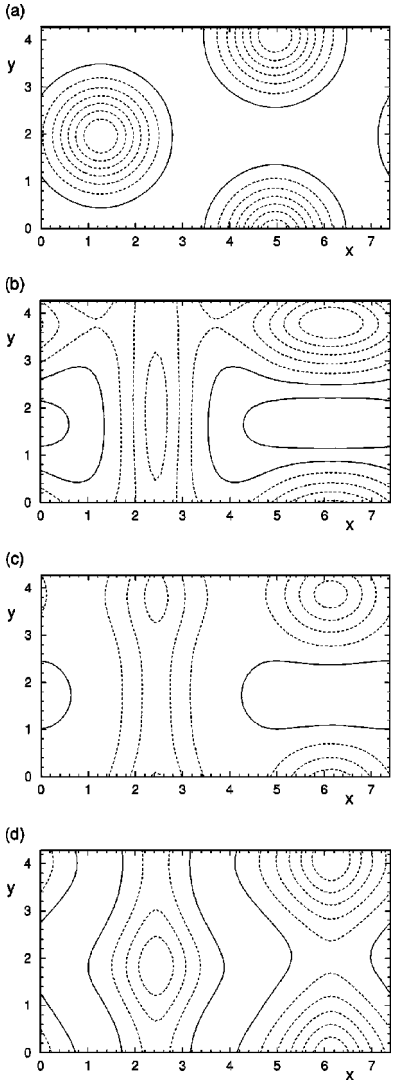

FIG. 1. Contour plots of θ at the free surface of the fluid layer. Panel (a): hexagons for $Ma=59$. Panel (b): $Ma=73$, $\tau=209.82$; Panel (c): $Ma=73$, $\tau=210.46$; Panel (d): $Ma=73$ $\tau=211.02$.

tional domain. Figure 1 illustrates this kind of oscillatory behavior for $Ma=73$ through several snapshots of the spatial distribution of θ on the top free surface $z=1$ (dotted lines correspond to negative θ). The roll-like structure arises when the deformed hexagon shrinks and vanishes when the hexagon expands. Characteristic of this oscillatory state is that the mean velocity field **V** is zero. The further changes in the pattern with increasing Marangoni numbers are connected with the excitation of the mean velocity field, which has the components $U(z)=\langle v_x\rangle_{x,y}$; $V(z)=\langle v_y=\rangle_{x,y}$ with corresponding total kinetic energies,

$$E_U=\int dzU^2(z), \quad E_V=\int dzV^2(z). \tag{4}$$

The development of the pattern for $Ma>66$ is as follows. First of all by means of a period-doubling bifurcation an oscillatory state connected to the mean field velocity component $V(z)$ arises. Concerning $U(z)$, the interval of Marangoni numbers can be divided in two subintervals with respect to $Ma=73.5$. Below this value $U(z)$ is practically zero. Above $Ma=73.5$ $U(z)$ increases that leads to increasing E_U. As can be seen from the lower two panels of Fig. 2, E_U increases slowly up to $Ma=74$ and has an irregular behavior. For higher Ma we observe intermittent behavior of $U(z)$ and E_U, and at the same time the amplitude of E_U rapidly becomes of the same order as the amplitude of E_V (see the lower right-hand side panel of Fig. 2). E_V has a different behavior (see upper and middle panels of Fig. 2). It oscillates periodically with increasing amplitude from $Ma=66$ to $Ma=70$. Then the oscillations become chaotic, e.g., at $Ma=72$. Above this value the oscillation amplitude decreases and the oscillations become again periodic. At $Ma=73$ the amplitude of the (periodic) oscillations is almost the same as the amplitude for $Ma=66$. The periodically oscillating pattern at $Ma=73$ shown in Fig. 1 drifts in the y direction, which, however, cannot readily be seen from the snapshots of a single oscillation period. With increasing Ma beyond 73 we observe a sharp increase in the oscillation amplitude up to $Ma=74$ and irregular behavior of the kinetic energy E_V with time. When $Ma>74$ E_V oscillates cha-

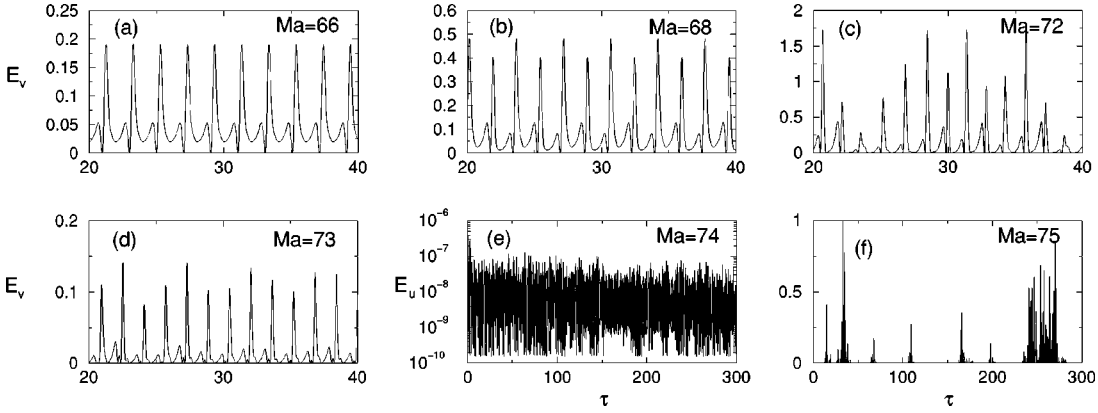

FIG. 2. Time behavior of the kinetic energy connected to the mean flow velocity components $V(z)$ and $U(z)$.

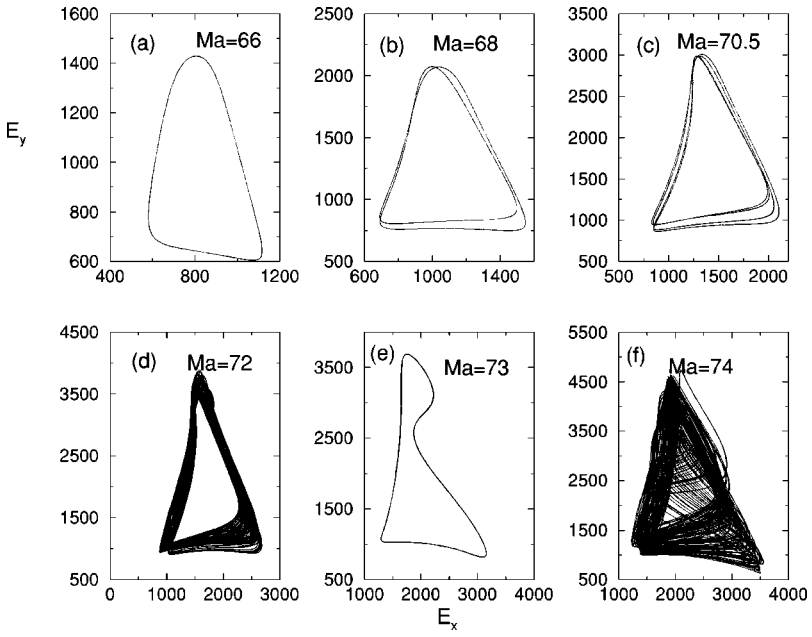

FIG. 3. Energy attractors for different values of the Marangoni number.

otically but the amplitude of the oscillations increases slowly in comparison with the large increase between $Ma=73$ and $Ma=74$.

In summary, the main difference between the chaotic states with $Ma<73$ and chaotic states with $Ma>73$ is that, in the former case only the mean field velocity component $V(z)$ is significantly different from zero whereas in the latter case both components of the mean field velocity are significantly large.

In order to obtain additional information on the behavior of the system for $Ma>66$ we shall now discuss the properties of the total kinetic energy of the fluid,

$$E_k=\frac{\rho}{2}\int_\Omega d\Omega(v_x^2+v_y^2+v_z^2)=E_x+E_y+E_z, \qquad (5)$$

where $E_{x,y,z}$ are the components of the kinetic energy in direction of the corresponding coordinate axes. The energy attractors for different values of the Marangoni number are presented in Fig. 3. For $66<Ma<71$ the development of the attractor follows a period-doubling scenario of the transition to chaos. For $Ma=71$ and above the attractor is a chaotic one (see the panel for $Ma=72$ in Fig. 3). With further increasing of Ma we observe a window of periodic motion and beyond this window the energy attractor becomes increasingly chaotic.

The considerable changes in the energy attractor do not lead to a complicated behavior of the mean kinetic energy of the system. There is an almost linear increase of the mean kinetic energy with Ma and the upper panel of the same figure shows that the mean kinetic energy in the direction of the z axis remains almost a constant fraction of the mean total kinetic energy. There exists about 3% difference between the mean values of E_x and E_y with E_y being larger for $Ma<70$. The situation is reversed at $Ma\approx80$. The transition region from E_y to E_x being larger coincides with the region of the chaotization of the energy attractor for the case of Marangoni numbers about 72 and with the region of the periodic window around $Ma=73$.

The system spends much of its time in vicinity of certain levels of the total kinetic energy. These levels can be seen as peaks in the histograms of the corresponding time series. In the case of a periodic motion the corresponding histogram usually has two peaks per loop, corresponding to the two points in which vicinity the attractor trajectory spends much more time than in the vicinity of the other points. In most cases these points are around the minimum and maximum values of the kinetic energy (as in the first three panels of Fig. 4). For the discussed system, however, we observe an additional dominant energy level almost in the middle of the interval between the energy levels near which the phase point spends much of its time in the phase space. This additional level can be seen very clearly in the panel for $Ma=73$ of Fig. 4 and it exists in a latent form even at $Ma=66$. When Ma increases beyond 73 the lowest and the highest dominant energy levels lose their unique status and the histogram looks more like a Gaussian.

Despite the complicated dynamics of the system energy two of the frequencies connected to the energy time series are more important than the other frequencies. This can be seen by an analysis of the power spectral density $S(f)=|H(f)|^2+|H(-f)|^2$, $0\leqslant f\leqslant\infty$ where the total power P of the signal $h(t)$ can be expressed by its Fourier transform $H(f)$: $P=\int_{-\infty}^{\infty}dt|h(t)|^2=\int_{-\infty}^{\infty}df|H(f)|^2$. We use discrete sampled data with time interval Δ and the unit for frequency is the Nyquist critical frequency $f_c=1/(2\Delta)$ that in our case is 100 (dimensionless units). The power spectral density is concentrated in the lower region of the power spectrum. Up to $Ma=73$, i.e., in the regions of the periodic motion, the first chaotization, and the periodic window we have one and the same dominant frequency $f_1=0.0057f_c$. With the beginning of the final chaotization of the energy attractor the dominant frequency shifts slightly to the right to the value $f_2=0.0077f_c$. When Ma increases further the power spec-

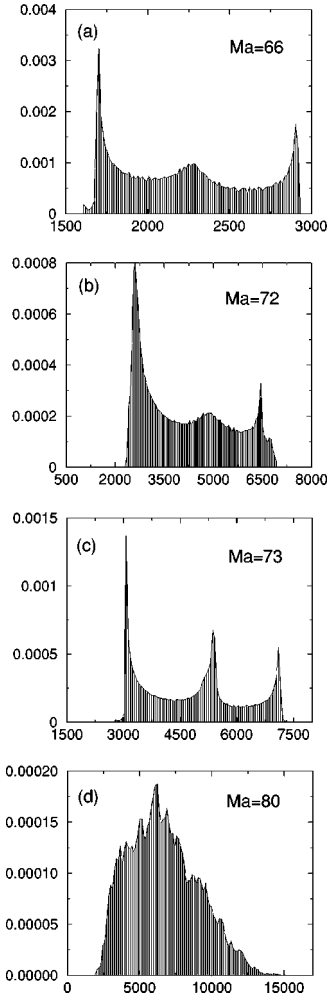

FIG. 4. Characteristic histograms for the total kinetic energy.

tral density disperses but nevertheless up to $Ma=80$, a large amount of power spectral density is still concentrated in the above-mentioned two frequencies and the power spectral density concentrated at f_1 becomes larger that the power spectral density at f_2.

The cross-correlation functions C_{xy}, C_{xz}, C_{yz} of E_x and E_y point to another difference between the chaotic states around $Ma=72$ and the chaotic states for $Ma>73$. Even when the time is quite advanced the cross correlations between the kinetic energies for the states around $Ma=72$ oscillate almost periodically with relatively large amplitude, whereas, in the case of the final chaotization of the attractor the behavior of the cross correlations is irregular and their amplitude tends to zero. We note that at $Ma=72$ the large amplitude of the oscillations of the cross-correlation function is a consequence of the strong influence of unstable periodic orbits on the attractor. With the final chaotization for $Ma>74$ the influence of such orbits decreases and thus, the amplitude of the oscillations of the cross-correlation function decreases, too. Therefore, the cross correlations have the typical form for chaotic time series for $Ma=78$ and larger.

Two important characteristics of the chaotic attractors are the maximum Lyapunov exponent and the correlation dimension [15–17]. For chaotic states the maximum Lyapunov exponent must be positive and the correlation dimension must be greater than 2. Indeed the maximum Lyapunov exponent has small positive values in the interval of Marangoni numbers between 74 and 80. The correlation dimension increases steadily from 2.09 at $Ma=74$ to 2.25 at $Ma=80$.

In this paper we present the results of a numerical study of the dynamics of BMC at zero Prandtl number in the basic rectangular domain containing two perfect hexagons at the onset of convection. Upon increasing the Marangoni number Ma we observe a complex picture of oscillating and drifting hexagons and roll-like structures and a transition to chaos accompanied by a nonzero mean field velocity field with component $U(z)$ exhibiting intermittent behavior around $Ma=75$. The kinetic energy attractor follows a period-doubling scenario of transition to chaos. We find a periodic window around $Ma=73$. The chaotic states below $Ma=80$ are strongly influenced by unstable periodic orbits.

We are grateful to the Zentrum für Hochleistungsrechnen of Dresden University of Technology for access to its parallel computing resources.

[1] M.F. Schatz and G.P. Neitzel, Annu. Rev. Fluid Mech. **33**, 93 (2001).
[2] S.H. Davis, Annu. Rev. Fluid Mech. **19**, 403 (1987)
[3] S. Schiller, U. Heisig, and S. Panzer, *Electron Beam Technology* (Wiley, New York, 1982).
[4] A. Pumir and L. Blumenfeld, Phys. Rev. E **54**, R4528 (1996).
[5] H.C. Kuhlmann and H.J. Rath, J. Fluid Mech. **247**, 247 (1993).
[6] M. Levenstam and G. Amberg, J. Fluid Mech. **297**, 357 (1995).
[7] A. Zebib *et al.*, Phys. Fluids **28**, 3467 (1985).
[8] T. Boeck and A. Thess, J. Fluid Mech. **350**, 149 (1997).
[9] T. Boeck and A. Thess, J. Fluid Mech. **399**, 251 (1999).
[10] O. Thual, J. Fluid Mech. **240**, 229 (1992).
[11] While inappropriate for experiments, the assumption of stress-free bottom turned out to be useful in earlier work [8]. It allows one to study the bifurcation to two-dimensional flywheel convection in its pure form. Moreover, a detailed study of the transition to chaos for no-slip conditions requires higher numerical resolution and is, therefore, more expensive computationally [9].
[12] J.H. Curry, J.R. Herring, J. Loncaric, and S.A. Orszag, J. Fluid Mech. **147**, 1 (1984).
[13] C. Canuto, M. Y. Hussaini, A. Quarteroni, and T. Zang, *Spectral Methods in Fluid Dynamics* (Springer, New York, 1988).
[14] D. Gottlieb and S. A. Orszag, *Numerical Analysis of Spectral Methods* (SIAM, Philadelphia, 1977).
[15] H. Kantz, Phys. Lett. A **185**, 77 (1994).
[16] P. Grassberger and I. Procaccia, Physica D **9**, 189 (1983).
[17] R. Hegger, H. Kantz, and T. Schreiber, Chaos **9**, 413 (1999).